International Journal of Applied Engineering Research ISSN 0973-4562 Volume 10, Number 17 (2015) pp 38509-38525

Development of Mathematical Models for Prediction of Weld Bead Geometry of Hardfaced Steel

Pratibha Kumari
Associate Professor and Research Scholar*
Mechanical Engineering Department
Krishna Institute of Engineering & Technology,
Ghaziabad.
karwalpratibha@gmail.com

R.P. Singh
Associate Professor
Mechanical Engineering Department
*GLA University,
Mathura
rudra.singh@gla.ac.in

Abstract-Hardfacing is a technique in which deposition of material on the surface of similar/dissimilar material is done to improve its wear resistant properties. The benefits also include the minimization of downtime needed to replace worn components and reduction of spare part inventory and finally saves money. So, it is essential to select welding process parameters carefully, to achieve a quality bead which is defect free. In order to achieve the above objective, a set of mathematical models has been developed for the prediction of weld bead geometry using 5-factor, 2 – levels Factorial design for 140MXC Nano composite wire with IS2062 steel as base plate. The developed models were checked for their adequacy. The main and the interaction effects of the process parameter on weld bead geometry are presented in graphical form.

Keywords: Harfacing**,** Gas Metal Arc Welding; Factorial Design Approach.

Introduction

Hrabe et al. (2009) stated that, in the field of welding, weld surfacing is one of the most economical method which saves time and money in conserving and extending the service life of engineering components. Weld surfacing increases the resistant to abration, corrosion, erosion etc. and is extensively used in chemical and fertilizer plants, pressure vessels, railways, mining, agriculture, etc. Under, weld surfacing , hardfacing can be defined as the application of wear resistant material on the surface of the components by weld overlay or thermal spray Halling, (1976), Wu and Wu, (1986),. Choteborsky et al. (2011) stated various methods used in weld surfacing as: Shielded Metal Arc Welding (SMAW), Submerged Arc Welding (SAW), Tungsten Inert Gas (TIG), Gas Metal Arc Welding (GMAW), Flux Cored Arc Welding (FCAW) etc. GMAW is extensively used for weld surfacing due to its high reliability, all position capability, ease of use, low cost, high productivity, high deposition rate, cleanliness and ease of mechanization as mentioned by Kannan and Yoganandh, (2010). All the major commercial metals can be welded by GMAW (MIG/CO2) process, including carbon steels, low alloy and high alloy steels, stainless, aluminium, and copper titanium, zirconium and nickel alloys illustrated by Singla et al .(2010).

Weld bead shape as shown in figure 1, plays an important role in determining the quality and mechanical strength of the weldment. Weld bead geometry is dependent on number of input parameters such as wire feed rate, welding speed, voltage, nozzle to plate distance, gas flow rate etc. as stated by Finney D. J.(1945), Cary H. B. (1979), Essers W. G. and Walter R. (1981), Cornu J.(1988), Kim et al.,(2003).

Hence, it is important to optimize these input parameters to get a good quality weldment with great mechanical properties. This may be attained by developing a mathematical model, which gives the welder a parametric window for operation.

Statistical approach is one way to increase the amount of information-rich data gathered. This approach has been employed by many researchers McGlone, (1982) and Metzbower, (1993). Numerous studies validated that efficient use of statistical design of experiment techniques, works as an excellent tool for the development of a mathematical model for the prediction of weld bead geometry, (Murugan and Parmer 1997, Subramaniam 1999), Allen et al.(2002), Kim et al.(2003).

So, to achieve the above mentioned objective stastical designing technique was employed to depict weld bead geometry of surfaced steel. Experiments were conducted based on fractional factorial designing i.e., 2 level 5 factors.

Developed mathematical models have been checked for their adequacy and significance.

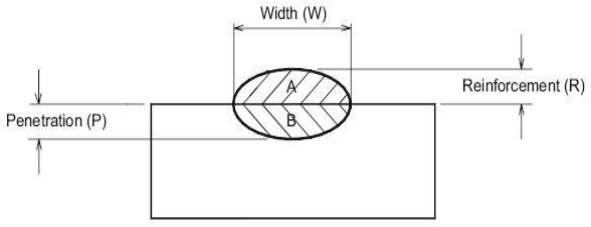

Fig. 1- Weld Bead Geometry

Experimental Work

The experiments were carried out by the deposition of 140MXC Nano-structured wire of 1.6 mm diameter using Miller Migmatic 273 welding machine. IS2062 used as base plate, was cut in 250 x 150 x 10mm size with some allowances for grinding etc. The chemical composition of base plate and filler wire are given in Table 1. Shielding gas

used was pure Argon with flow rate kept constant at 25 l/min. Bead- on – plate technique was used to make the weld runs.

Table 1 Chemical composition of base plate and filler wire.

IS 2062						
Element	**C**	**Si**	**Mn**	**S**	**P**	**Fe**
%	**0.227**	**0.161**	**0.50**	**0.05**	**0.023**	**Balance**

TAFA 140MXC Nano-structured wire							
Element	**Cr**	**C**	**Mo**	**B**	**W**	**Si**	**Nb**	**Fe**
%	**20.8**	**2.84**	**12.1**	**0.64**	**9.79**	**0.54**	**0.8**	**Balance**

Plan of Investigation

The research work was planned to be carried out in the following steps:
(i) identifying the important process control variables; (ii) determining the upper and the lower limits of the control variables; (iii) developing the design matrix; (iv)conducting the experiments as per the design matrix; (v) recording the responses, viz. penetration (P), weld width (W), reinforcement (R), and dilution (D); (vi) developing the mathematical models; (vii) calculating the coefficients of the polynomials; (viii)checking the adequacy of the models; (ix) testing the significance of the regression coefficients and arriving at the final mathematical models; (x) presenting the main effects and the significant interactions between the different parameters in graphical form. Kumari et. al (2011), Srimath and Murugan(2011).

1. Identifying the important process control and response variables

Wire feed rate, welding speed, welding voltage, nozzle to plate distance and torch angle were chosen as process control variable. Response variable chosen were penetration (p), bead width (w), crown height (h) and % dilution (%D).

2. Determining the Upper and Lower levels for the input variables

To determine the two levels of each control variables, pilot study was carried out by varying the control variables in all possible combination. The experiments so carried, gave the limits, which is shown in table- 2.

Welding parameters were coded as (+1) and (-1), corresponding to the high and low levels for the ease of recording and processing of the data using equation (1).

$$X_j = (X_{jn}-X_{jo}) \ / J_j \qquad (1)$$

Where, X_j is the coded value of the parameter, X_{jn} is the natural value of the parameter, X_{jo} is the natural value of the basic level, J_j is the variation interval and j is the number of parameter.

Table 2 Levels of the welding parameters.

Parameters	Units	Symbols	Lower Limit -1	Upper Limit +1
WireFeed Rate	m/min	W	7.62	9.04
Welding Speed	cm/min	S	27	36
Voltage	Volts	V	26	32
Nozzle to Plate Distance	mm	N	15	20
Torch Angle	Degree	T	80	100

3. Developing the design matrix

Factorial design can be written in the form of a design matrix where the rows correspond to different trials and the columns correspond to the levels of the process parameters. The design matrix developed to conduct the eight trials of 2^n fractional factorial design is given in table-3.

Table 3 Design matrix

Experiment No.	W 1	S 2	V 3	N 4	T 5= -(1234)
1	-1	-1	-1	-1	-1
2	1	-1	-1	-1	1
3	-1	1	-1	-1	1
4	1	1	-1	-1	-1
5	-1	-1	1	-1	1
6	1	-1	1	-1	-1
7	-1	1	1	-1	-1
8	1	1	1	-1	1
9	-1	-1	-1	1	1
10	1	-1	-1	1	-1
11	-1	1	-1	1	-1
12	1	1	-1	1	1
13	-1	-1	1	1	-1
14	1	-1	1	1	1
15	-1	1	1	1	1
16	1	1	1	1	-1

4. Conducting the experiments as per the design matrix

From the design of the experiments, it was clear that 16 trials were needed to run, keeping the values set in the design matrix. The weld runs were then performed on each of these strips throughout the length of the strip using the Miller magmatic 273 welding machine as shown in Figure 2, in DCEP polarity. The weld runs were made in the sequence in order to avoid confusion and were marked alphabetically using chalk and later with letter punch stencils. Figure 3 shows the bead-on-plate of the specimen.

Fig. 2 Setup of GMAW unit

Fig. 3 Bead-on-plate of the specimen

5. Recording the responses, viz. penetration (p), weld width (w), reinforcement (h), and dilution (D)

Three samples each of about 10mm-15mm were cut by using a slitting cutter on universal milling machine after discarding 50 mm of the bead length from either end. A sample of the cut pieces are shown in the figure 4. All the test specimens were ground and polished. Polishing was carried out as per the metallurgical practice on a set of five emery papers (400, 600, 800, 1000, 1200 grit) changing successively the direction of polishing by 90^0 when moved from rougher to finer emery. This was done in order to eliminate completely the polishing marks produced by previous emery. Now to get the distinguished view between the HAZ and weld bead geometry the samples were etched with Nital solution: 3% HNO_3 and 97% CH_3OH. Some of the specimens are shown in figure 5. The etching procedure involved dipping of the test piece in etchant at for 5-10 minutes, followed by tap water rinsing and finally hot air drying.

.

Figure 4 Sample cut out after welding

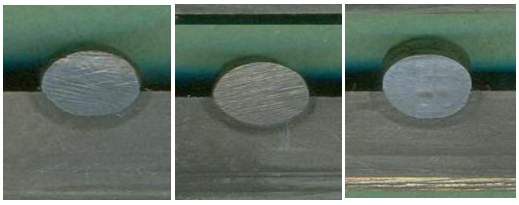

Figure 5 Sample cut out after etching

To get the dimensions of the bead geometry all the samples were scanned on their original size. The scanned images were then transferred to Corel Draw X5, using the ruler tool in the software the dimensions were measured and tabulated as shown in Table 4.

Table 4 Bead geometry mean response

EXPMT No.	W m/min	S cm/min	V V	N mm	T degree	Width,w mm	Reinforcement height,H mm	Depth of Penetration,P mm	Dilution, % D
1	-1	-1	-1	-1	-1	8.4	4.4	4.6	40.01
2	1	-1	-1	-1	1	8.7	5.1	4.3	33.34
3	-1	1	-1	-1	1	5.5	4.1	3.2	34.7
4	1	1	-1	-1	-1	7	4.5	4	36.95
5	-1	-1	1	-1	1	11.5	3.9	4.5	44.25
6	1	-1	1	-1	-1	10.5	4.1	4.1	33.9
7	-1	1	1	-1	-1	7	3.4	3.1	38.25
8	1	1	1	-1	1	10.8	3.0	4.2	50.86
9	-1	-1	-1	1	1	5.8	4.7	2.4	24.5
10	1	-1	-1	1	-1	6.8	5.1	5.1	39.61
11	-1	1	-1	1	-1	7	3.7	2.6	32.6
12	1	1	-1	1	1	6.5	3.6	3.6	42.29
13	-1	-1	1	1	-1	10.7	3.6	4.9	52.56
14	1	-1	1	1	1	13.7	3.7	4.1	41.60
15	-1	1	1	1	1	7.2	3.4	4.6	53.46
16	1	1	1	1	-1	9	3.8	3.3	36.69

6. Selection of a mathematical model

The response function y, representing the welding responses, could be represented as:

$y = f(W, S, V, N, T)$ (2)

Where the responses variable, 'y' were penetration (p), bead width (w), crown height (h) and % dilution (%D) respectively. The direct process parameters W, S, V, N and T represent the wire feed rate, welding speed, welding voltage, nozzle to plate distance and torch angle respectively.

Assuming a linear relationship in the first instant and taking into account all the possible two-parameter interactions, the above expression can be expressed as:

$y = b_0+b_1W+b_2S+b_3V+b_4N+b_5T+ b_6 WS+b_7 WV+b_8 WN+b_9 WT+b_{10} SV+b_{11} SN+ b_{12} ST+b_{13} VN+b_{14} VT+b_{15} NT$

Where, $b_0, b_1, b_2, \ldots\ldots\ldots\ldots b_{15}$ are the coefficients of the polynomial equation

7. Evaluation of coefficients and developing the mathematical models

Regression analysis was used for determining the coefficients of the model. The regression coefficients of the selected model were calculated using Equation (4)

$$bij = \frac{\sum_{i=1}^{M} X_{ji} Y_i}{M}, \; j = 0,1,2,3.....,k \quad (4)$$

Where, X_{ji} is the value of a parameter or interaction in coded form, Y_i is the average value of the response parameters, M is the number of observations and k is the number of coefficients of the model. (5)

These models for predicting different responses mentioned above are given below.

w= 8.51+ 0.62W - 1.01S + 1.54 V – 0.17N + 0.21T + 0.21WS + 0.33WV + 0.04WN + 0.59 WT - 0.54SV + 0.09 SN - 0.21ST + 0.27VN + 0.54VT - 0.24 NT (6)

h= 4.01 + 0.11W - 0.32S - 0.39V - 0.06N - 0.07T - 0.07WS -0.07WV - 0.01WN -0.19WT + 0.11SV - 0.01SN - 0.09ST + 0.07VN - 0.04VT - 0.03NT (7)

p= 3.91 + 0.18W - 0.34S + 0.19V - 0.09N - 0.05T + 0.03 WS - 0.35 WV + 0.03 WN + 0.01 WT + 0.04 SV + 0.04 SN + 0.38 ST + 0.21 VN + 0.30 VT - 0.1 NT (8)

%D= 39.72 - 0.32W + 1.0S + 4.22V + 0.69N + 0.9T + 1.29WS -2.87WV- 0.05WN +1.72WT - 0.13SV - 0.16SN + 3.7ST + 1.44VN+ 2.69VT - 0.85NT

8. Checking the adequacy of the models

The adequacy of the model and significance of the coefficients was tested by applying 'F' and student's't' test respectively Kumari et. al (2011) and Singla et al.(2010).The major aim of analyzing data from designed experiments is to quantify and evaluate the importance of possible source of variation. This can be achieved through Analysis of Variance (ANOVA) associated with the analysis of underlying model chosen as mentioned in table 5. To ensure the accuracy of the developed model and survey the spread of values, results were plotted using the scatter diagram. The scatter diagram for observed vs. estimated values of weld bead penetration, height, width and % dilution for different rows of the design matrix is given in figure 6 to figure 9 respectively.

Table-5 Analysis of variance (ANOVA).

Resp-onse	**DOF**		**Var. response**	**Std. dev.**	**Var. adeq.**	**'F' model**	**'F' table**	**F_m<F_t**
	S^2_Y	S^2_{ad}	S^2_Y	S_{bj}	S^2_{ad}	S^2_{ad}/S^2_Y	(10,16,0.05)	
w	16	10	0.310	0.139	0.031	0.10	2.49	Yes
h	16	10	0.330	0.143	0.033	0.10	2.49	Yes
p	16	10	0.080	0.07	0.008	0.10	2.49	Yes
%D	16	10	0.594	0.192	0.059	0.10	2.49	Yes

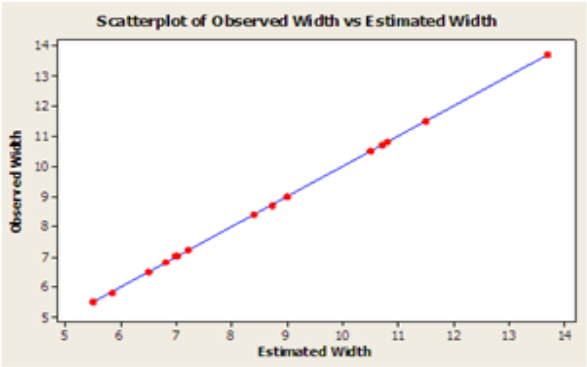

Fig. 6 Scatter plot of weld bead width model

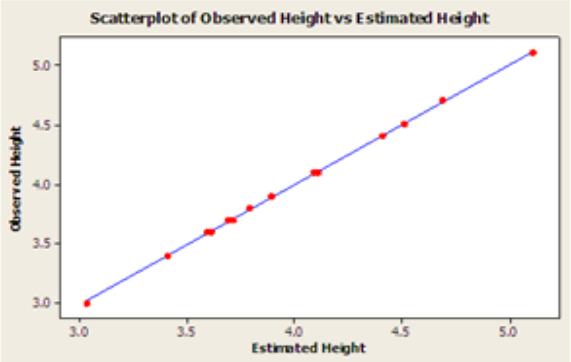

Fig. 7 Scatter plot of weld bead height model

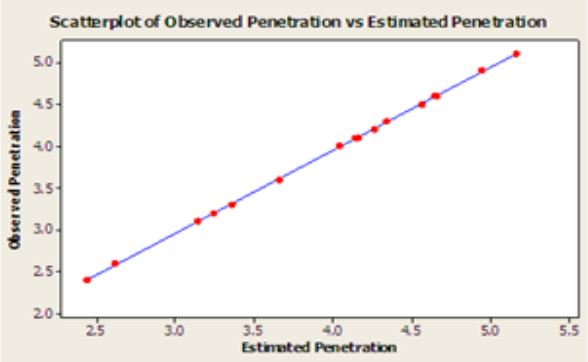

Fig. 8 Scatter plot of weld bead penetration model

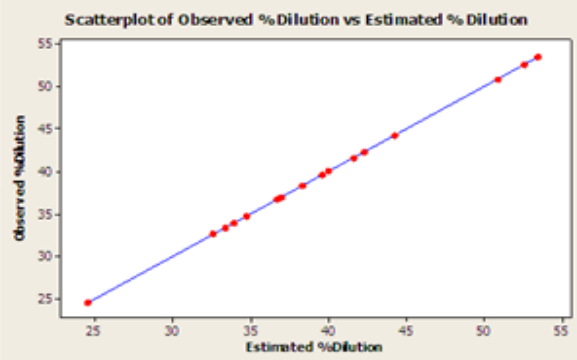

Fig. 9 Scatter plot of weld bead dilution model

9. Testing the significance of the regression coefficients and final proposed mathematical models

The proposed models developed for bead geometry after dropping insignificant coefficients are given in table 6 Kumari et al. (2011). Based on these models, graphs have been drawn for interpretation of the direct and interaction effects of the process parameters on bead geometry.

Table-6 Proposed models for bead geometry and shape relationships.

w= 8.51 + 0.62w-1.01S + 1.54V + 0.33 wV +0.59 wT -0.54 SV +0.54 VT – 0.24 NT
h= 4.01 -0.32S + -0.39V
p = 3.91 + 0.18W -0.34S + 0.19V -0.35 WV+ 0.38 ST + 0.21 VN+ 0.30 VT
%D= 39.72 -0.32W + 1.0 S + 4.22V -2.87 WV +1.72 WT -0.13 SV + 2.69 VT

10. Significant main effects and interactions

The variation of responses i.e. penetration, height, width and dilution with respect to the wire feed rate, welding speed, welding voltage, nozzle to plate distance and torch angle respectively are shown in, figure 10 to figure 13. The interaction effects of different input parameters on penetration, height, width and dilution are shown in figure 14 - figure 29.

Analysis of results

The mathematical models that were fitted to the experimental data provided satisfactory correlations. This is also evident from the scatter diagrams as shown in figure 6 to figure 9. The direct effect and interaction effect of various welding parameter on bead geometry were depicted by feeding the coded values in the final model of penetration, height, width and %dilution and

varying one input parameter at a time and keeping others at fixed value i.e gas flow rate at 25l/min, voltage at 32V, wire feed rate at 9.04 m/min, welding speed at 36 cm/min, nozzle to plate distance at 20mm and torch angle at 100^0 . The effects have been discussed as under:

1. Effect of voltage

Increase in voltage has the following effect on penetration, height, width and % dilution as shown in figure 10.

1. The weld penetration increased from 3.43mm to 4.83 mm.
2. The height decreased from 4.47 mm to 2.91mm.
3. The bead width increased from 4.73mm to 12.21 mm.
4. The % dilution increased from 34.3 to 49.94.

The penetration increases gradually with increase in voltage and reaches a maximum value. The height decreases with increase in voltage but the reverse is true with the width and dilution. Increasing the arc voltage makes the bead wider; the height is reduced because the same volume of weld metal is involved. Greatest effect of individual parameter on bead width was of arc voltage. The increase in arc voltage resulted in the increase in bead width from 4.73 mm to 12.21 mm. This increase in bead width could be attributed to the increased arc length with rise in arc, which resulted in large spread of the arc at its base and hence increased weld width. The increase in arc voltage also results in hotter arc, which means high fluid state of the deposited metal.

2. Effect of wire feed rate

Increase in wire feed rate has the following effect on penetration, height, width and % dilution as shown in figure 11.

1. The weld penetration increased from 4.31 mm to 4.99 mm.
2. The height remains constant at 3.33mm.
3. The bead width increased from 5.72 mm to 11.88 mm.
4. The % dilution decreased from 50.44 to 44.56.

The penetration increases gradually with increase in wire feed rate and reaches a maximum value. Wire feed has very little or no effect on height within the operating range of the present investigation. It can be noted that an increase in wire feed rate results in significant increase in the bead width. Increase in wire feed rate results in higher fluidity of the molten wire which in turns gives higher deposition rate which could be attributed for this increase in bead width. For a good joint dilution should be as small as possible. Increase wire feed rate results in decrease in dilution but has very small effect.

3. Effect of welding speed

Effect of increase in welding speed on penetration, height, width and %dilution, as shown in figure 12, is as follows:

1. The weld penetration increased from 4.36 to 4.52 mm.
2. The height decreased from 4.26 mm to 2.98 mm.
3. The bead width decreased from 14.99 mm to 8.79 mm.
4. The % dilution increased from 43.42 to 46.9.

As the welding speed is inversely proportional to depth of penetration, the depth of penetration should decrease with increase in the welding speed. But the result shows the reverse trend. This is mainly due to the fact that, there is a critical range for welding speed, beyond which the penetration increases with increase of welding speed. As the welding speed increases, the depth of penetration increases up to an optimum level and then decreases with further increase in welding speed. Another reason behind this behavior could be that with low welding speed, the arc is almost vertical and in this instance, the weld pool cushions the effect of arc and prevents deeper penetration. Increase in speed has a marked effect on bead width and height. This could be due to the fact that weld pool size is affected by cooling rate which can decrease by decreasing the travel speed. Thus at high speed, size of the weld pool will be less i.e. width and height will decrease. Dilution increased with increase in welding speed. However, in comparison with wire feed rate, the rate of increase of dilution was significantly low.

4. Effect of nozzle to plate distance

Increase in nozzle to plate distance has the following effect on penetration, height, width and %dilution as shown in figure 13.

1. The weld penetration increased from 3.85 mm to 4.69 mm.
2. The height remains constant at 3.3mm.
3. The bead width decreased from 11.06mm to 10.1 mm.
4. The % dilution remains constant at 46.03.

As the nozzle to plate distance increases, the depth of penetration increases. which may be due to higher temperature of the droplets impinging on the weld pool because of more resistance heating of the wire at higher nozzle-to-plate distances. Nozzle to plate distance has no effect on reinforcement height and dilution. With increase of nozzle to plate distance, width decreases a bit. This is due to the fact that with increase in nozzle to plate distance, welding current drops and this drop results in reduced base metal melting and reduction in weld bead width.

5. Effect of torch angle

Increase in torch angle has the following effect on penetration, height, width and %dilution as shown in figure 14.

1. The weld penetration increased from 2.44 mm to 5.16 mm.
2. The height remains constant at 3.3.
3. The bead width increased from 7.67 mm to 11.23 mm.
4. The % dilution increased from 32.8 to 50.44.

It can be noted that weld width and penetration increases significantly with increase in torch angle

from 80^0 to 100^0. i.e. from backhand to forehand welding. This could be due to the fact that electic arc produces an electrical force known as arc force. This arc force is able to put more pressure when torch is kept at higher angle. The results also match with the study of Mostafa and Khajavi (2006).Torch angle does not show any significant change in height. Dilution increases when the angle increases.

6. Interaction between wire feed rate and voltage

Figure 15 to Figure 18 shows the response surface due to the interaction of wire feed rate and voltage on penetration, height, and width and % dilution and the effect is as follows:

1. Width is highest with the wire feed rate of 9.04 m/min and voltage of 32 V and least at wire feed rate of 7.62 m/min and voltage of 26 V.
2. Reinforcement height was found to be maximum at a voltage of 26 V while wire feed rate do not shows any effect.
3. Penetration increases with increase in wire feed rate but at high voltage of 32 V, penetration increases abruptly with increase in wire feed rate.
4. With the increase in voltage from 26 V – 29 V, dilution was found to increase but beyond this voltage i.e. for 29 V – 32 V, it was noted that there was decrease in dilution.

7 Interaction between wire feed rate and torch angle

Figure 19 to Figure 22 shows the response surface due to the interaction of wire feed rate and torch angle on penetration, height, and width and % dilution. The effects are discussed as as follows:

1. Penetration is highest with a torch angle of 100^0 and wire feed rate of 7.62 m/min and least at a torch angle of 80^0 and wire feed rate of 9.04 m/min.
2. Interaction of wire feed rate and torch angle does not show any effect on reinforcement height.
3. Width increases with increase in torch angle of 100^0 and is highest at the wire feed rate of 9.04 m/min but at a torch angle of 80^0, a slight decrease of width was seen for a increase in wire feed rate from 7.62 m/min to 9.04 m/min.
4. Dilution decreases with decrease in torch angle but at a lower angle of 80^0 Dilution decreases abruptly with increase in wire feed rate from 7.62 m/min to 9.04 m/min.

8 Interaction between welding speed and voltage

Figure 23 to Figure 26 shows the response surface due to the interaction of welding speed and voltage on penetration, height, and width and % dilution as follows:

1. Penetration increased very slightly with increase in welding speed but had a peak value at a voltage of 32 V.
2. Reinforcement height was found to be highest for a welding speed and voltage of 27 cm/min and 26 V respectively. It was lowest at welding speed and voltage of 36 cm/min and 32 V respectively with a decreasing slop.
3. Width was seen to be highest at a welding speed and voltage of 27 cm/min and 32 V respectively. It shows a slight increase in width at a voltage of 26 V when welding speed increases from 27 cm/min to 36 cm/min.
4. Dilution had a greater effect when voltage was kept at 26 V but peak value can be achieved at a welding speed and voltage of 36 cm/min and 32 V respectively.

9 Interaction between welding speed and torch angle

Figure 27 to Figure 30 shows the response surface due to the interaction of welding speed and torch angle on penetration, height, and width and % dilution as follows:

1. Penetration decreases abruptly with increase in welding speed and at a torch angle of 80^0 . It was noted that there was increase in penetration with increase in torch angle i.e. at 100^0 for any value of welding speed.
2. Reinforcement height was found to be decreasing with increase in welding speed at all the degrees of torch angle.
3. At a torch angle and welding speed of 100^0 and 27 cm/min respectively width was seen to be highest but was least for a torch angle and welding speed of 80^0 and 36 cm/min respectively
4. Dilution was noted to be maximum when torch angle and welding speed were kept at 100^0 and 36 cm/min respectively

10 Interaction between voltage and nozzle to plate distance

Figure 31 to Figure 34 shows the response surface due to the interaction of voltage and nozzle to plate distance on penetration, height, and width and % dilution as follows:

1. At a nozzle to plate distance of 15mm, penetration was noted to decrease abruptly with increase in voltage. Further, it was noted that there was increase in penetration with increase in nozzle to plate distance from 18.75 mm – 20mm.
2. Interaction of voltage and nozzle to plate distance does not show much effect on reinforcement height.
3. At a voltage and nozzle to plate distance of 26V and 20mm respectively width was seen to be highest but was least for a voltage and nozzle to plate distance of 32V and 15mm respectively.
4. Interaction of voltage and nozzle to plate distance does not show much effect on dilution.

11 Interaction between voltage and torch angle

Figure 35 to Figure 38 shows the response surface due to the interaction of of voltage and torch angle on penetration, height, and width and % dilution as follows:

1. At a torch angle of 80^0, penetration was noted to decrease abruptly with increase in voltage. Further, it was noted that there was increase in penetration with increase in torch angle from 90^0 - 100^0.
2. Interaction of voltage and torch angle had a similar kind of decreasing effect on reinforcement height.
3. Width increases with increase in voltage but at a torch angle of 100^0 it was noted that width increases abruptly with increase in voltage.
4. At a torch angle of 80^0, dilution was noted to decrease abruptly with increase in voltage. Further, it was noted that there was increase in penetration with increase in torch angle from 90^0 - 100^0.

12 Interaction between nozzle to plate distance and torch angle

Figure 39 to Figure 42 shows the response surface due to the interaction of of nozzle to plate distance and torch angle on penetration, height, and width and % dilution as follows:

1. Penetration increased very slightly with increase in nozzle to plate distance and was found to be at peak at a torch angle of 100^0.
2. Interaction of nozzle to plate distance and torch angle does not show much effect on reinforcement height.
3. With a increase in torch angle from 80^0 - 90^0, width was noted to increase with increase in nozzle to plate distance but this angle i.e. from 90^0 - 100^0, it was noted that there was decrease in width.
4. Interaction of nozzle to plate distance and torch angle does not show much effect on dilution.

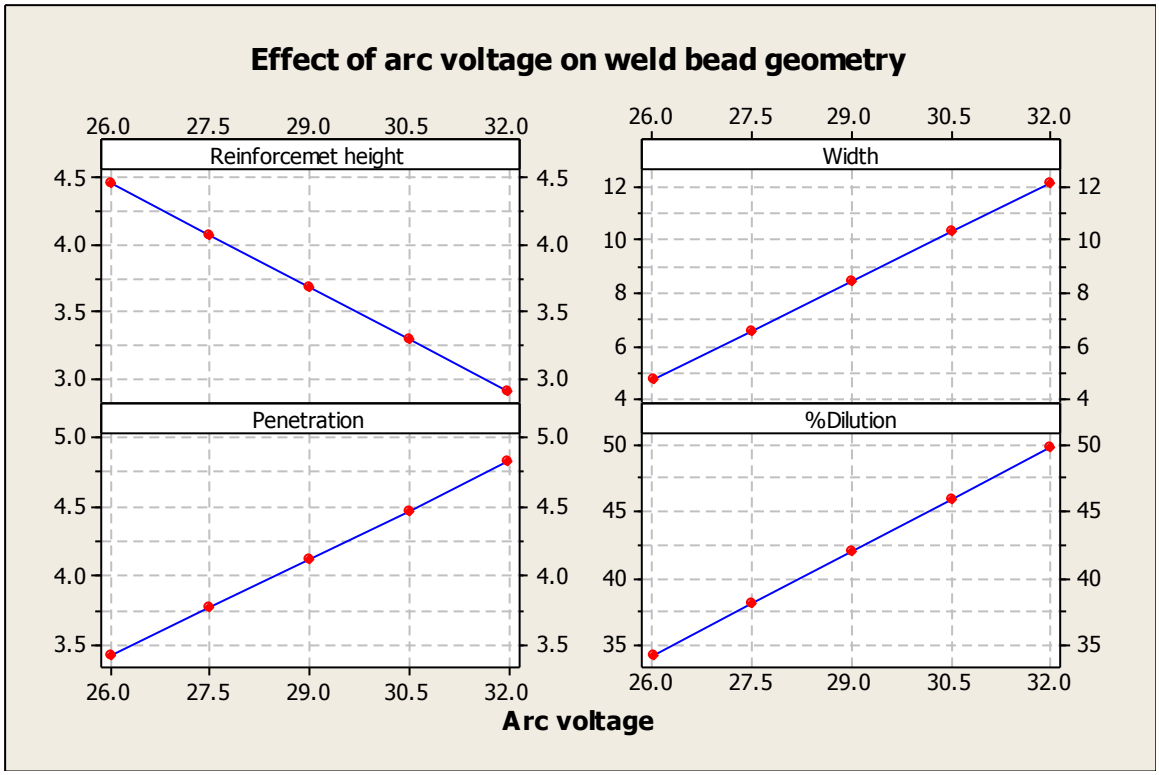

Figure 10 Effect of voltage on penetration, reinforcement height, width, % dilution

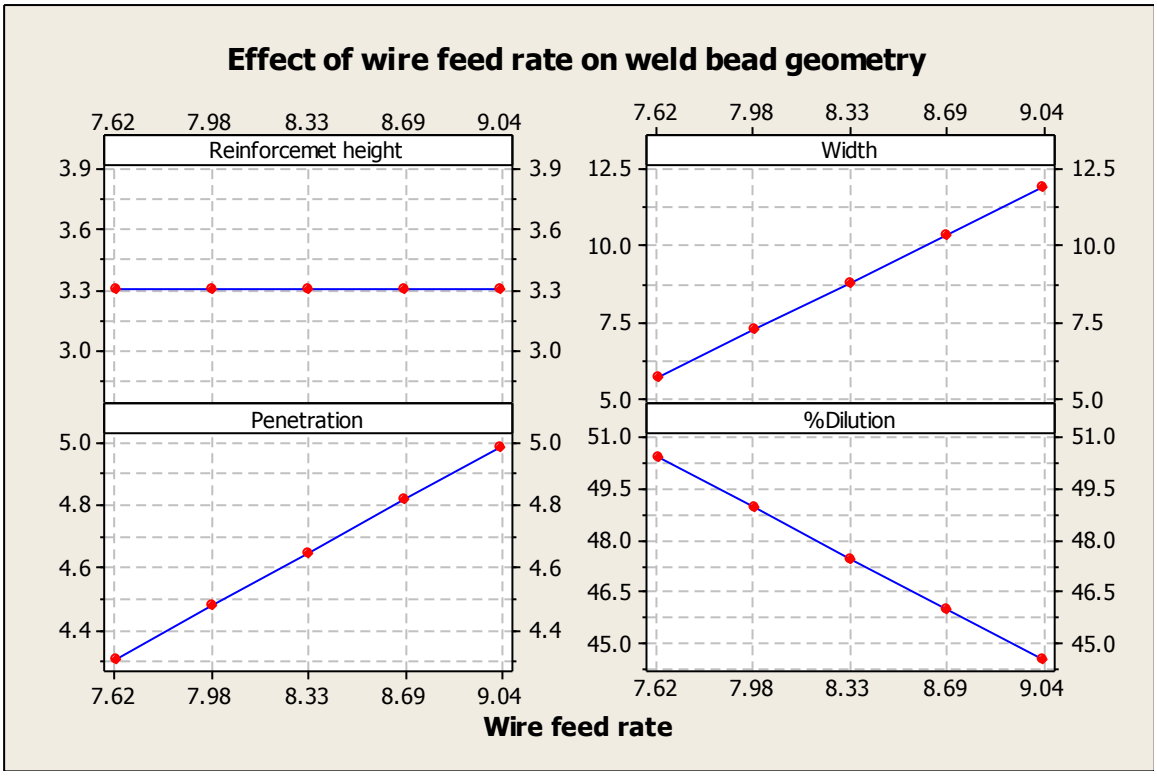

Figure 11 Effect of wire feed rate on penetration, reinforcement height, width, %dilution

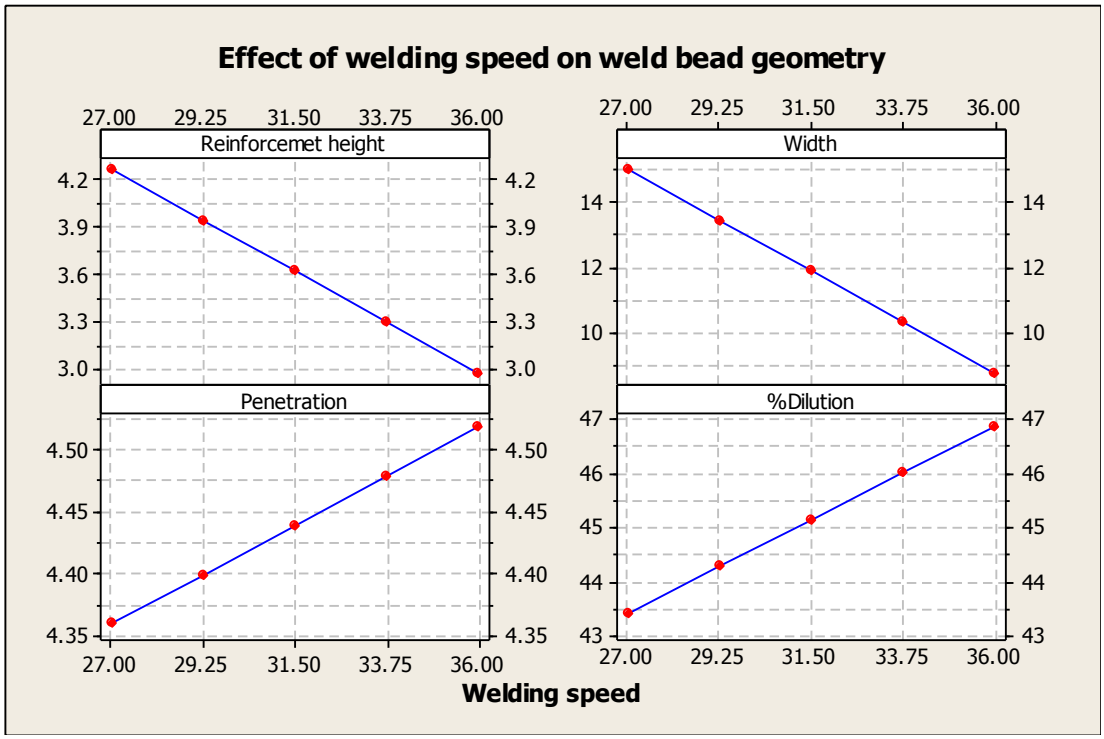

Figure 12 Effect of welding speed on penetration, reinforcement height, width, %dilution

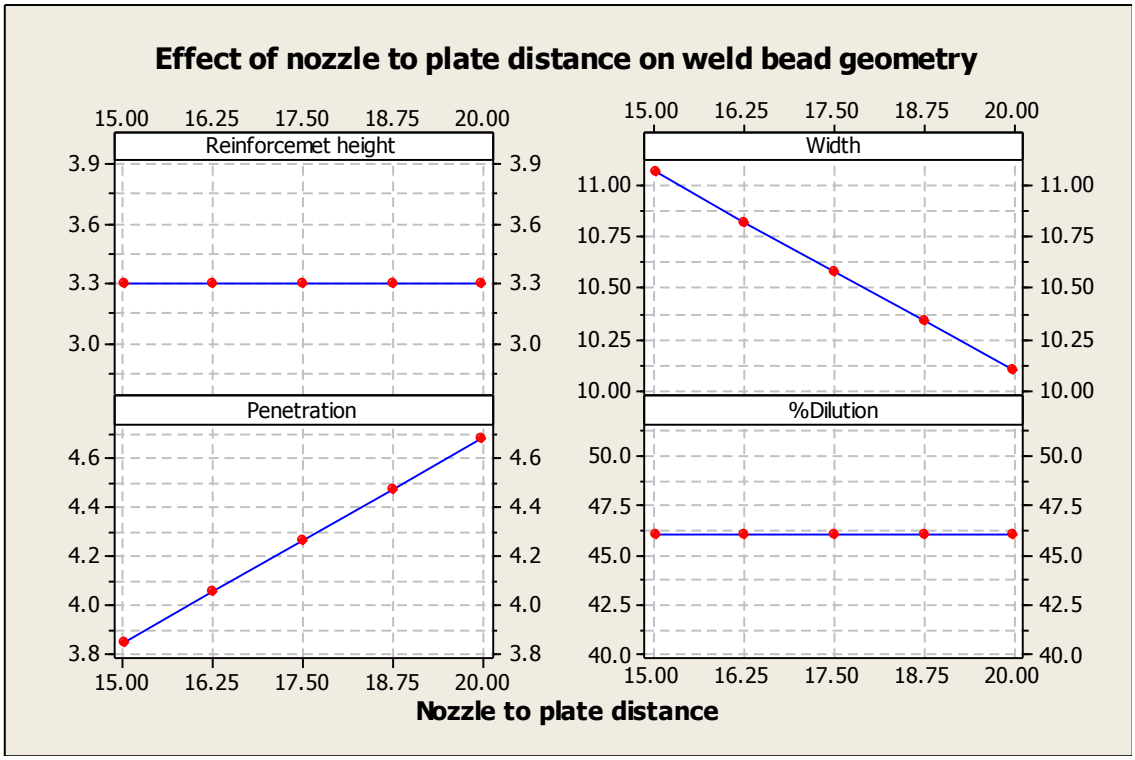

Figure 13 Effect of nozzle to plate distance on penetration, reinforcement height, width, %dilution

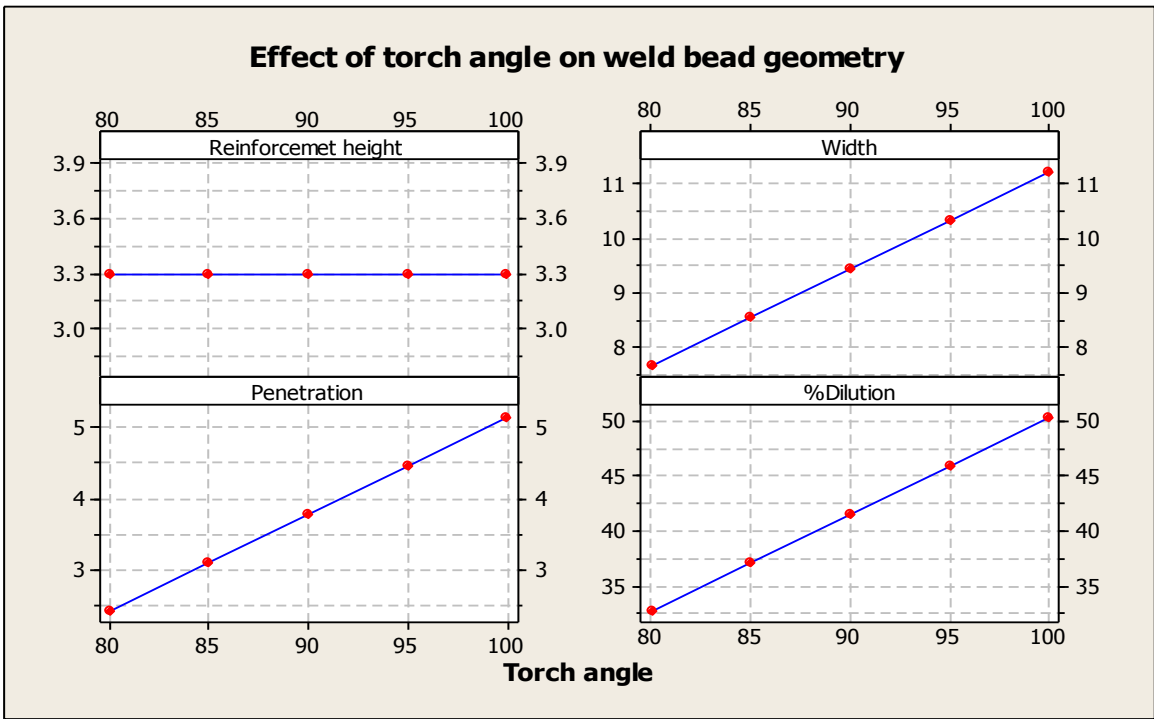

Figure 14 Effect of torch angle on penetration, reinforcement height, width, %dilution

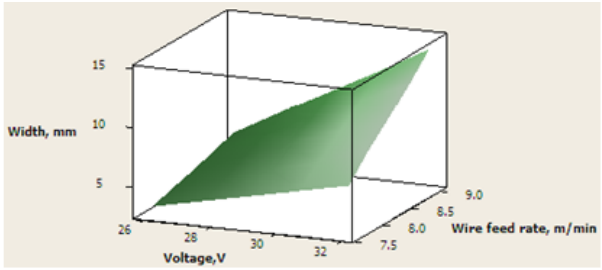

Figure 15 Response surface on width due to an interaction of wire feed rate and voltage

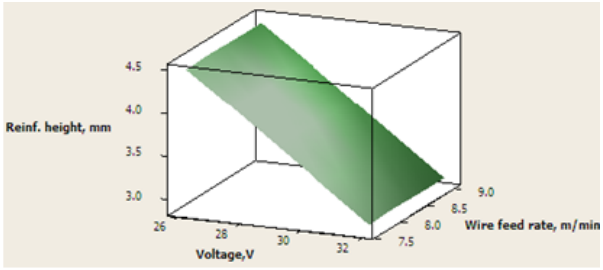

Figure 16 Response surface on reinforcement height due to an interaction of wire feed rate and voltage

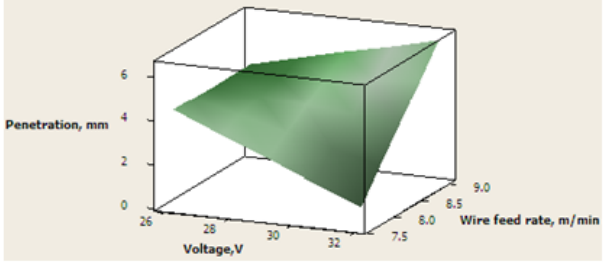

Figure 17 Response surface on penetration due to an interaction of wire feed rate and voltage

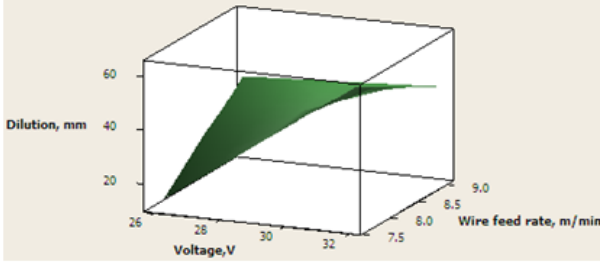

Figure 18 Response surface on dilution due to an interaction of wire feed rate and voltage

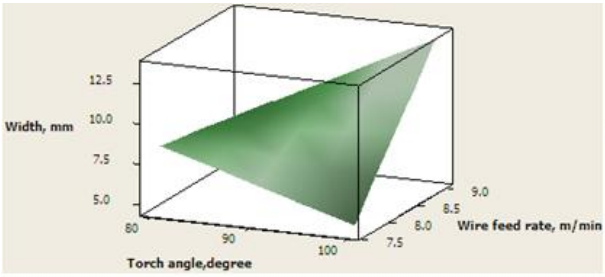

Figure 19 Response surface on width due to an interaction of wire feed rate and torch angle

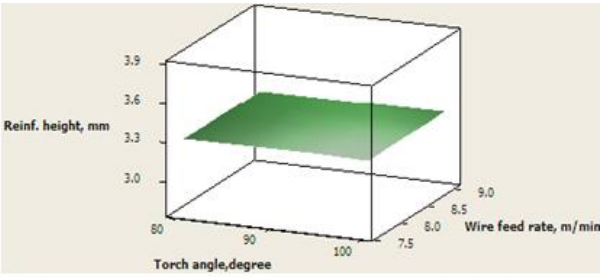

Figure 20 Response surface on reinforcement height due to an interaction of wire feed rate and torch angle

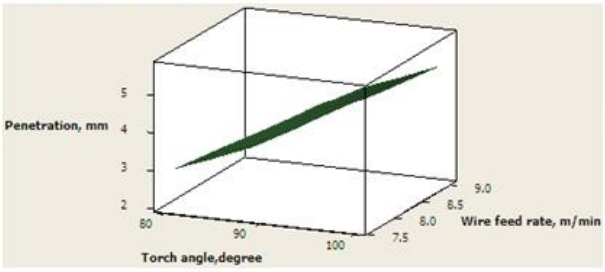

Figure 21 Response surface on penetration due to an interaction of wire feed rate and torch angle

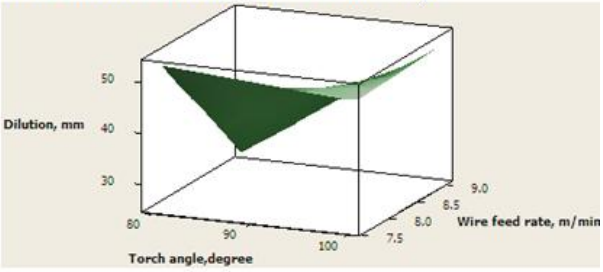

Figure 22 Response surface on dilution due to an interaction of wire feed rate and torch angle

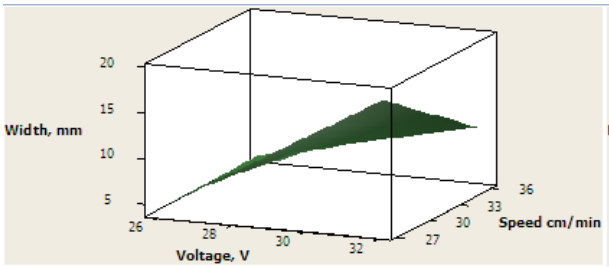

Figure 23 Response surface on width due to an interaction of speed and voltage

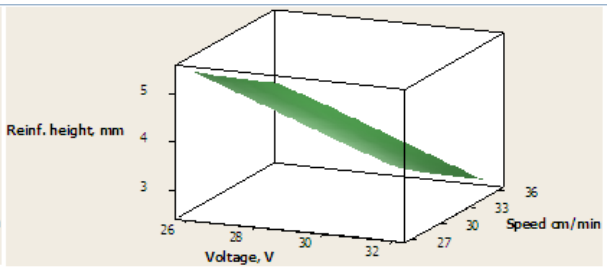

Figure 24 Response surface on reinforcement height due to an interaction of speed and voltage

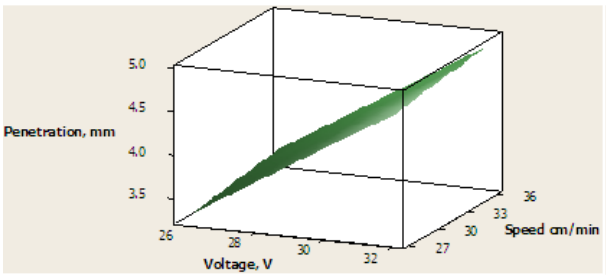

Figure 25 Response surface on penetration due to an interaction of speed and voltage

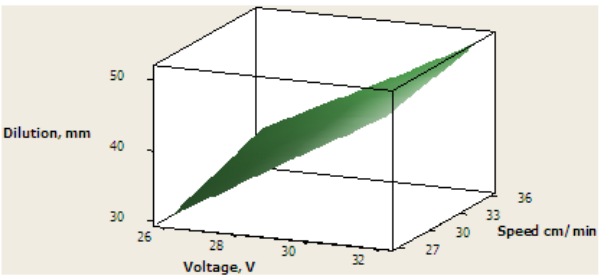

Figure 26 Response surface on dilution due to an interaction of speed and voltage

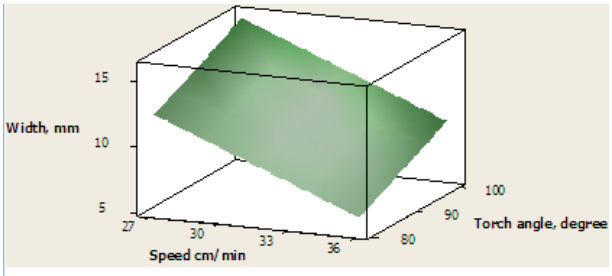

Figure 27 Response surface on width due to an interaction of speed and torch angle

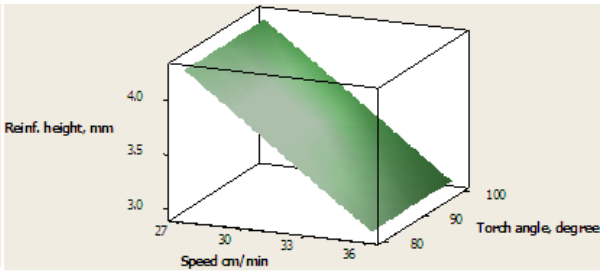

Figure 28 Response surface on reinforcement height due to an interaction of speed and torch angle

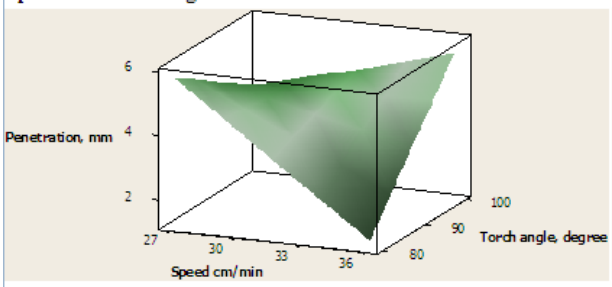

Figure 29 Response surface on penetration due to an interaction of speed and torch angle

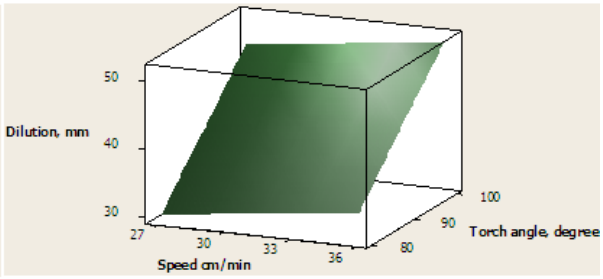

Figure 30 Response surface on dilution due to an interaction of speed and torch angle

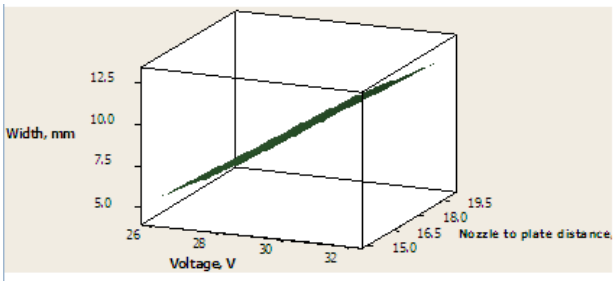

Figure 31 Response surface on width due to an interaction of nozzle to plate distance and voltage

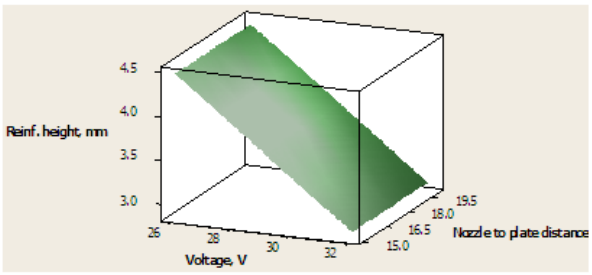

Figure 32 Response surface on reinforcement height due to an interaction of nozzle to plate disatance and voltage

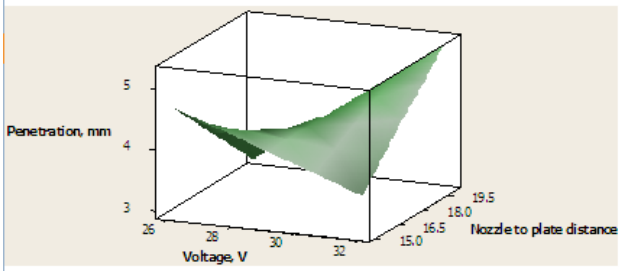

Figure 33 Response surface on penetration due to an interaction of nozzle to plate disatance and voltage

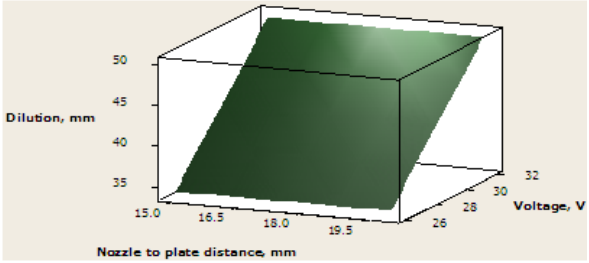

Figure 34 Response surface on dilution due to an interaction of nozzle to plate distance and voltage

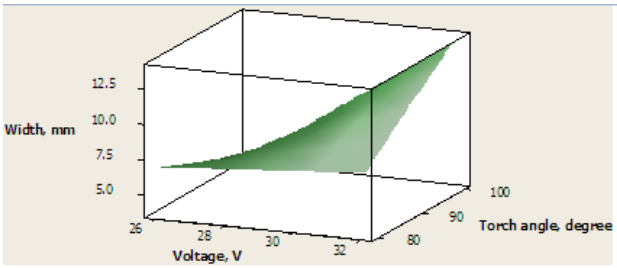

Figure 35 Response surface on width due to an interaction of voltage and torch angle

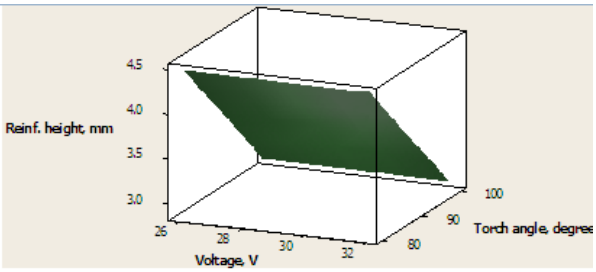

Figure 36 Response surface on reinforcement height due to an interaction of voltage and torch angle

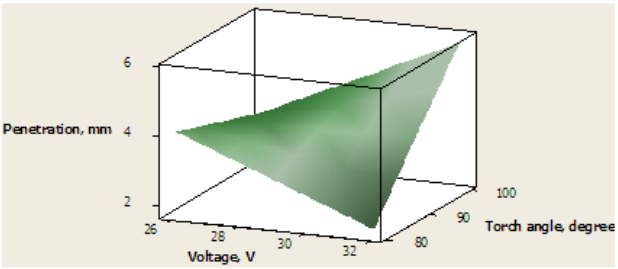

Figure 37 Response surface on penetration due to an interaction of voltage and torch angle

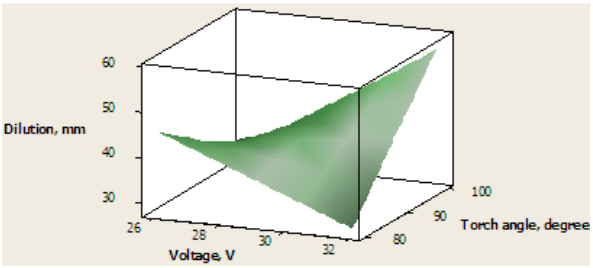

Figure 38 Response surface on dilution due to an interaction of voltage and torch angle

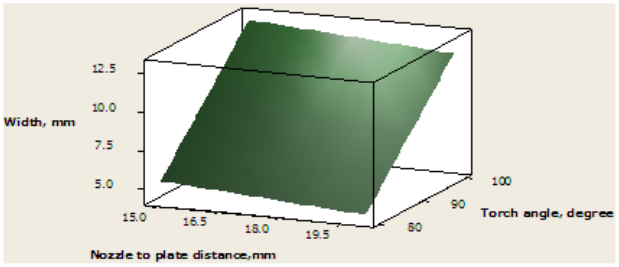

Figure 39 Response surface on width due to an interaction of nozzle to plate distance and torch angle

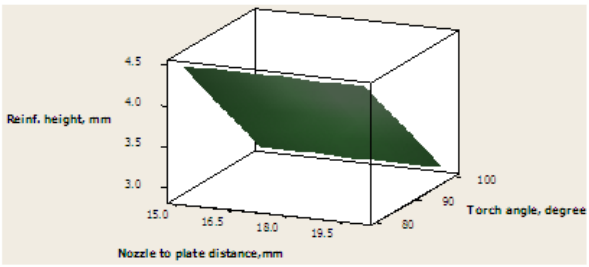

Figure 40 Response surface on reinforcement height due to an interaction of nozzle to plate distance and torch angle

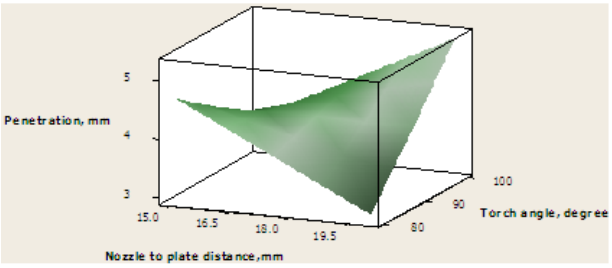

Figure 41 Response surface on penetration due to an interaction of nozzle to plate distance and torch angle

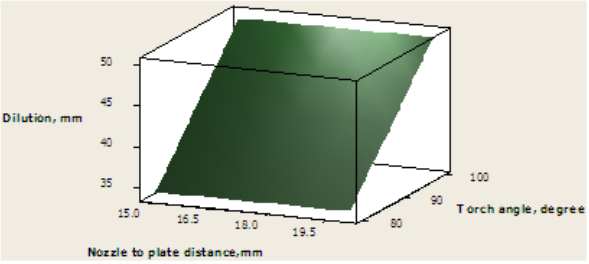

Figure 42 Response surface on dilution due to an interaction of nozzle to plate distance and torch angle

Conclusion

The conclusions are drawn from the study of mathematical models as well as the experiments conducted in actual condition. Important results are as follows:

1. Response surface methodology (RSM) approach is an excellent and effective tool, for the development of mathematical model for the prediction of response.
2. Scatter diagram ensures the accuracy of the model.
3. Increase in voltage from 26V to 32V resulted in increase of penetration, width and dilution. Reinforcement height decreased with increase in voltage.
4. Increase in wire feed rate from 7.62m/min to 9.04m/min results in increase of penetration, width. Dilution decreased with increase in wire feed rate. Reinforcement height remains unaffected.
5. Increase in speed from 24cm/min to 36cm/min resulted in slight increase of penetration and dilution. Reinforcement height and width decreased significantly with increase in speed.
6. Increase in nozzle to plate distance from 15mm to 20 mm resulted in increase of penetration, width decreased with increase in voltage. Reinforcement height and dilution remains unaffected.
7. Interaction of speed and torch has the most dominant effect on bead width.
8. Interaction of wire feed rate and torch angle; nozzle to plate distance and torch angle gives the minimum height of 3.3mm.
9. Interaction of wire feed rate and voltage gives the maximum penetration of 6.39mm.
10. % Dilution of 45.6 seems to be minimum with the interaction of wire feed rate and voltage.

References

[1] Allen, T.T., Richardson, R.W., Tagliabue, D.P. and Maul, G.P., 2002. Statistical process design for robotic GMA welding of sheet metal. Weld J. 81(5): pp 69s–76s.

[2] Cary, H. B., 1979. Modern Welding Technology. New Jersey, Prentice Hall, pp 169-175.

[3] Choteborsky, R., Navratilova, A. and Hrabe, P., 2011. Effects of MIG process parameters on the geometry and dilution of the bead in the automatic surfacing. Res. Agr. Eng., 57: 56–62. Vol. 57, No. 2: pp 56–62.

[4] Cornu, J., 1988. Advanced Welding Systems-Part2., London, IFS Limited, pp 168.

[5] Essers, W. G. and Walter, R., 1981. Heat transfer mechanisms with GMA and plasma-GMA welding. Welding Journal (3): pp 69-76.

[6] Finney, D. J., 1945. The fractional replication of factorial arrangement., Annals of Eugenics (12): pp 291-301.

[7] Halling, J., 1976. Introduction to Tribology, University of Salford, pp 42-46.

[8] Hrabe, P., Choteborsky,R. and Navratilova, A., 2009. Influence of welding parameters on geometry of Weld deposit bead. in: Proceedings of the International Conference on Economic Engineering and Manufacturing Systems. Brasov, pp 26 – 27.

[9] Kannan, T. and Yoganandh, J., 2010. Effect of process parameters on clad bead geometry and its shape relationships of stainless steel claddings deposited by GMAW. Int. J Adv Manuf. Technol. 47: pp 1083–1095.

[10] Kim, I.S., Son, J.S., Kim, I.G., Kim, J.Y. and Kim, O.S., 2003. A study on relationship between process variables and bead penetration for robotic CO2 arc welding. Journal of Materials Processing Technology 136, pp 139-145.

[11] Kumari, P., Archana, K., Parmar,R.S.,2011.Effect of Welding Parameters on Weld Bead Geometry in MIG Welding of Low Carbon Steel. International Journal of Applied Engineering Research.6(2): pp. 249–258.

[12] McGlone, J. C., 1982. Weld bead geometry prediction-A review, Metal Construction 14(7): pp 378-384.

[13] Metzbower, A. E., 1993. Penetration depth in laser beam welding. Welding Journal (8): pp 403-407.

[14] Murugan, N. and Parmar, R. S., 1997. Effect of welding conditions on microstructure and properties of tupe 316L stainless steel submerged arc welding cladding. Weld J., AWS 1997;76(5): pp 210-s–20-s.

[15] Singla, M., Singh, D. and Dharmpal, D., 2010. Parametric Optimization of Gas Metal Arc Welding Processes by Using Factorial Design Approach. *Journal of Minerals & Materials Characterization & Engineering*, Vol. 9, No.4, pp.353-363.

[16] Srimath, N. and Murugan, N., 2011. Prediction and Optimization of Weld Bead Geometry of Plasma Transferred Arc Hard faced Valve Seat Rings. European Journal of Scientific Research Vol.51 No.2, pp.285-298.

[17] Subramaniam, S., White, D. R., Jones, J. E. and Lyons, D. W., 1999. Experimental approach to selection of pulsing parameters in pulsed GMAW, AWS. Weld J. 78(5): pp 166-s–172-s.

[18] Wu,W. and Wu, L.T., 1986. The Wear Behaviour between Hardfacing Materials, *Metall. Mater. Trans. A*, Vol 27, pp 3639-3646.